Int J Adv Manuf Technol (2012) 58:1043–1050
DOI 10.1007/s00170-011-3428-x

ORIGINAL ARTICLE

The effect of welding parameters on fracture toughness of resistance spot-welded galvanized DP600 automotive steel sheets

Fatih Hayat · İbrahim Sevim

Received: 29 November 2010 / Accepted: 20 February 2011 / Published online: 14 June 2011

Abstract The aim of this study was to evaluate the fracture toughness of resistance spot welded (RSW) lap joints of galvanized DP600 steels. RSW lap joints galvanized DP600 steel sheets were performed on spot welded in a pneumatic, phase-shift-controlled, and 0–9 kA effective weld current capable AC spot welding machine. Defect-free RSW lap joints were produced on galvanized DP600 steel sheets. Fracture toughness of RSW lap joints were calculated from the results of shearing tensile tests: the dependence of fracture toughness to welding current, welding time, and hardness of welding zone for galvanized DP600 steel sheets. According to the experimental data, the fracture toughness increases as welding current and welding time increase up to a certain value, then the fracture toughness starts to decrease. Also, it was seen that the fracture toughness varies with the hardness of the welding zone. This variation is related to welding current.

Keywords Resistance spot welding · Dual phase (DP) steels · Fracture toughness · Welding current · Welding time

İ. Sevim
Mechanical Engineering Department,
Engineering Faculty, Mersin University,
33343 Ciftlikkoy-Mersin,
Mersin, Turkey
e-mail: ibrahimsevim33@gmail.com

F. Hayat (✉)
Metallurgy Materials Engineering Department,
Engineering Faculty, Karabuk University,
Baliklarkayasi,
78050 Karabuk, Turkey
e-mail: fatih-hayat@hotmail.com

1 Introduction

Advanced high-strength steels (AHSS) commonly have been used in the automotive body structures as automotive industry due to reduced vehicle weight, high strength, safety requirements, good corrosion resistance, and improved crash resistance [1–6]. Dual phase (DP) steels are one of the most common AHSS steels. DP steels, which consist primarily of a ductile ferrite phase and a strong martensite phase, provide excellent mechanical properties in commercial high-strength low-alloy steels. Compared with carbon steels, DP steels exhibit a number of unique mechanical properties such as slightly lower yield strength and more uniform and higher total elongation, which is responsible for their relatively good formability. These properties, combined with high strengths, have made DP steels attractive for automotive applications [7–10]. In recent years, DP600 applications are widely used in different automobile models such as Porsche Cayenne [11], Land Rover LR2 (http://myautoworld.com/auto/land_rover/landrover-08-lr2/landrover-08-lr2.html), and Jaguar XF (http://www.worldautosteel.org/Applications/Vehicles/Jaguar-XF.aspx). While the reported weight saving is 50% in the SAB report due to DP600, the reported weight reduction in the ULSAC report [12] was 46%. The SAB reported that a weight saving of 17.9% was due to reducing the material thickness in the rear side rails from 6.7 to 5.5 mm thickness by using DP600 steel. In 2002, Corus conducted a research that intended to reduce the weight of the vehicles without reducing the impact strength. This research reported that DP600 steel is the most axial crash and bending crash resistant steel after TRIP600 steel in durable steel ranking [13].

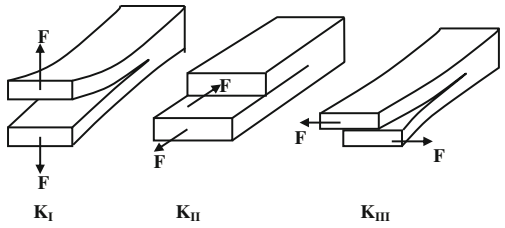

Fig. 1 Basic fracture modes: K_I opening mode; K_{II} shearing mode; K_{III} tearing mode [27]

DP steels are joined by several welding methods. Resistance spot welding (RSW) is the main joint method of assembly auto body due to its high efficiency in processing thin DP steel sheets. A wide variety of DP steel sheets up to 3 mm thickness can be handled by the RSW method. RSW for DP steels is the simplest, fastest, and most controllable. Hence, the automotive industry uses RSW at several thousand welding points in each automotive body structures [14–16].

The resistance spot welded joints of automobiles are subject to forces under the static and dynamic loads. The fatigue failure in the zones under dynamic loads is critical. Fatigue failure starts at a discontinuity or crack in the sample grows in time and the fracture occurs. Especially, the mechanical and metallurgical variations occur in the welding zone and the heated parts due to the fast heating and cooling of the welded zone after the resistance spot welding process. These variations considerably affect the strength of the welded spot under the dynamical forces. Welded zones have critical stress intensity for fatigue failure [17].

The factors such as shear stress acting in RSW zone, sheet thickness, multi pass welding, and the width of the welding zone are the important parameters that affect the performance of the joint. Stress intensity factor is used to express the fatigue life of spot welds. This quantity is used to predict the fatigue life of RSW. In order to determine the fracture parameters such as the notch stress at spot-welded joints and stress intensity factor, the fracture mechanics approach is employed [18, 19]. The fracture mechanics approach is commonly used to compute the stress intensity factors of the spot-weld joints under shear-tensile stress forces. The weak points in microstructure of the spot weld may trigger the fracture at the welding zone. The computation method for stress intensity factor using fracture mechanics is discussed briefly in following paragraphs [19].

The main purpose in the fracture mechanics analysis is to determine the fracture parameters, e.g., stress intensity factors. The fracture of a material is studied in three different modes [15]. These are opening mode K_I, shearing mode K_{II}, and tearing mode K_{III}, as seen in Fig. 1.

Little work has been done in establishing stress-intensity expressions for spot-welded sheets. Pook [20] investigated the fracture behavior of spot welds using the expressions developed by Paris, Sih, and Kassir [21, 22] based on elliptical connections, in spot-welded joints. Radaj [23] showed that the fatigue strength of spot-welded joints could be assessed considering the local stress. Zhang [24, 25] showed the relation between the stress intensity factor and the J integral for spot-welded joints. Zhang [24] introduced the following equations for the stress intensity factors K_{II} for spot-welded joints.

$$K_{\mathrm{II}} = \frac{2F}{\pi D\sqrt{S}} \quad \left(\mathrm{MPa.m}^{1//2}\right) \tag{1}$$

where D, S, and F denote the spot weld diameter, sheet thickness, and tensile-shear force, respectively.

In literature, there are studies which explain the mechanical properties of RSW. Wilson and Fine [26] defined the stress intensity. Pan and Sheppard [27] discussed the formation of capillary cracks in weld zone and tried to estimate the stress intensity factors for these capillary cracks. Darwish et al. [28] investigated failure rate of spot-welded joints depending on welding parameters. Chang et al. [29] investigated the hardness in the interface of the plates which were welded by lap joint spot welding. Chandel and Garber [30] formulated the strength of different spot weld microstructures (martensitic, bainitic, cold-rolled) according to the variations in the electrical current and welding cycle. Zuniga and Sheppard [31] showed that the tensile and yield strength changes with the hardness of the heat-affected zone of a zinc-coated high-strength low-alloy steel. Ma et al. [2] studied microstructure and fracture characteristics of spot-welded DP600 steel. Marya and Gayden [32] investigated weld fracture in relation to weld parameters and steel sheet characteristics. Baltazar Hernandez et al. [33] studied influence of microstructure and weld size on the mechanical behavior of dissimilar AHSS-resistant spot welds. However, there are limited studies, which investigate the fracture toughness of RSW joints. Lack of comprehensive study for assessing the fracture toughness of RSW joints has led to the present work to be carried out.

Table 1 Chemical composition of base metals (wt.%)

Specimen	C	Si	Mn	Cr	Ni	Nb	Ti	V	Mo	Fe
DP600	0.11	0.182	1,6	0,34	0.027	0.0037	0.002	0.0035	0.098	Bal.

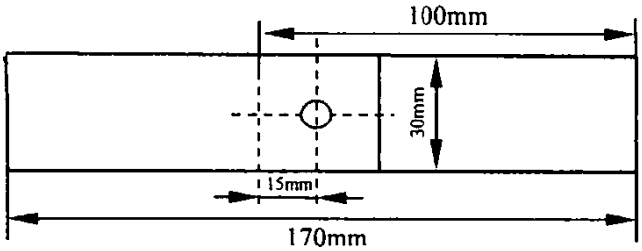

Fig. 2 The sizes of resistance spot-welded test specimens

The aim of this study is to investigate fracture toughness of galvanized DP600 steel sheets under RSW against the welding current and welding time. RSW lap joints galvanized DP600 steel sheets were performed on spot welded in a pneumatic, phase-shift-controlled, and 0–9 kA effective weld current capable AC spot welding machine. Defect-free RSW lap joints were produced on galvanized DP600 steel sheets. Fracture toughness of RSW lap joints were calculated from the results of shearing tensile tests: the dependence of fracture toughness to welding current, welding time, and hardness of welding zone for galvanized DP600 steel sheets.

2 Experimental procedure

A 1.20-mm thick zinc-coated DP600 steel (as-received) was used in the experiments. The thickness of galvanized dual phase steels used in experiments is 23 μm, and their chemical composition is given in Table 1.

Sheet with a thickness of 1.20 mm fabricated from the dual phase steel was subjected to spot resistance welding in a Baykal SPP60 installation. The dual phase steel sheet was cut into pieces in dimensions of 100×30 mm. This installation is an AC machine for spot welding equipped with a device for pneumatic control of the phase shift of the AC current. The power of installation was 60 kW. Before joining, the surface of the test pieces was cleaned mechanically and then welded using a conical water-cooled electrode from a Cu–Cr alloy. The diameter of the contact surface of the electrode was 8.0 mm. The specific force of pressing of the electrode were constant, as $F_{SP}=6\times10^5$ Pa. Welding processes were carried out by using 3–5–7–9 kA weld current and 10–20–30–40 cycles (1 cycle=0.02 s) weld time (Fig. 2).

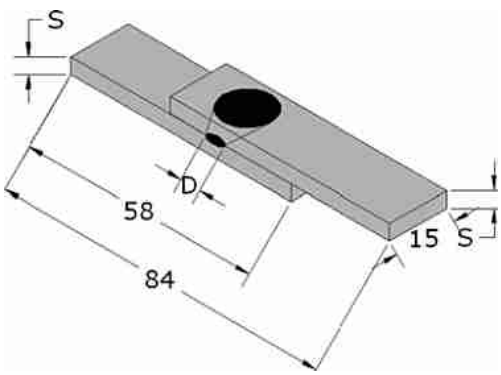

Fig. 3 Sizes of tensile-shear test specimens for device

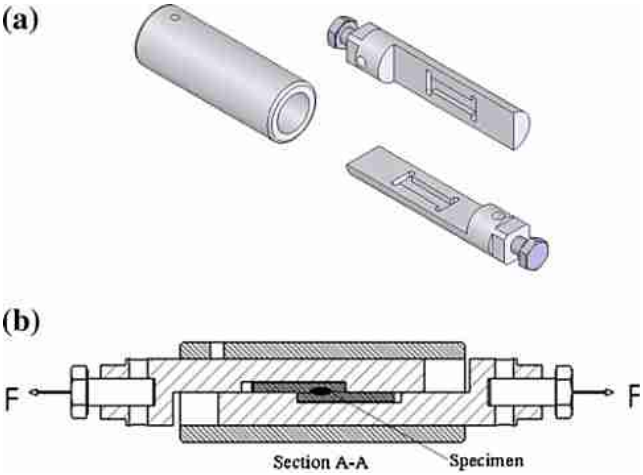

Fig. 4 Shearing tensile test device and shearing tensile test specimen: **a** three-dimensional model for device, **b** sectional view of shearing tensile test device

Fracture toughness of RSW lap joints were calculated from the results of shearing tensile tests. The dimensions of the shearing tensile test specimens that were machined from the FSW lap welded joints are given in Fig. 3. A special tensile shearing test device was designed and fabricated, as shown in Fig. 4a and b to perform shearing tensile tests on RSW lap joints. The spot-welded parts were tested under the tensile-shear mode as shown in Fig. 5. Tensile-shear load is taken as the maximum rupture load value. The spot-welded samples were exposed to tensile-shear test in

Fig. 5 View of tensile test machine

Fig. 6 Microstructure photograph of the galvanized DP600 specimen welded

Shimadzu UH 5,000 kN type testing machine in laboratory conditions. The crosshead speed was kept constant 2 mm min^{-1} during tests.

The fracture force of the welded parts was determined from the data obtained in the tensile-shear tests. The nugget diameters were measured from the optical microscopy taken from the fracture surface of the samples which were pulled to failure in the shearing mode. Three measurements were performed for each of the sample. Mean values of the measurements were taken as nugget diameter. Equation 1 was used to calculate the fracture toughness values (K_{IIC}).

The heat-affected zone of the spot weld was ground using abrasive papers of 80–1,200 meshes and then polished with 0.3 μm diamond paste (see Fig. 6). The micro-hardness of the polished surface was measured at the load of 1.96 N (HV0.2).

3 Results

As shown in Fig. 7, when the weld current is increased, the fracture toughness increases until a critical weld current. After that value, fracture toughness decreases because of the excessive melting and splashing.

Table 2 A and B constants in the variation of fracture toughness with welding current

Weld time t (second)	The equations for K_{IIC}	Constant, A	Constant, B
0,2	$K_{IIC} = 8.05 \times 10^{-3} I - 5 \times 10^{-7} I^2$	8.05×10^{-3}	5×10^{-7}
0,4	$K_{IIC} = 7.85 \times 10^{-3} I - 5 \times 10^{-7} I^2$	7.85×10^{-3}	5×10^{-7}
0,6	$K_{IIC} = 7.65 \times 10^{-3} I - 5 \times 10^{-7} I^2$	7.65×10^{-3}	5×10^{-7}
0,8	$K_{IIC} = 7.45 \times 10^{-3} I - 5 \times 10^{-7} I^2$	7.45×10^{-3}	5×10^{-7}

The estimated variation of fracture toughness with welding current is a decreasing second-degree polynomial curve (Fig. 7). This plot demonstrates that the welded galvanized DP600 steel sheets have three different zones (see Fig. 7):

I. Zone The welding at low welding currents and short welding time; in this zone, the current and time is insufficient for the formation of weld nucleus. This zone includes the welding currents up to 4 kA.

II. Zone This zone corresponds to the welding currents of 4–8 kA (Fig. 7). In this zone, the welding current and welding time are sufficient to form the weld nucleus. The fracture toughness has the maximum values in this zone. Weldability is best in this zone.

III. Zone Welding current (I) and welding time (t) have extreme values in this zone. Despite the increase of welding current and welding time, the fracture toughness decreases. The welding current is larger than 8 kA. The welded spot scatters and has cracks.

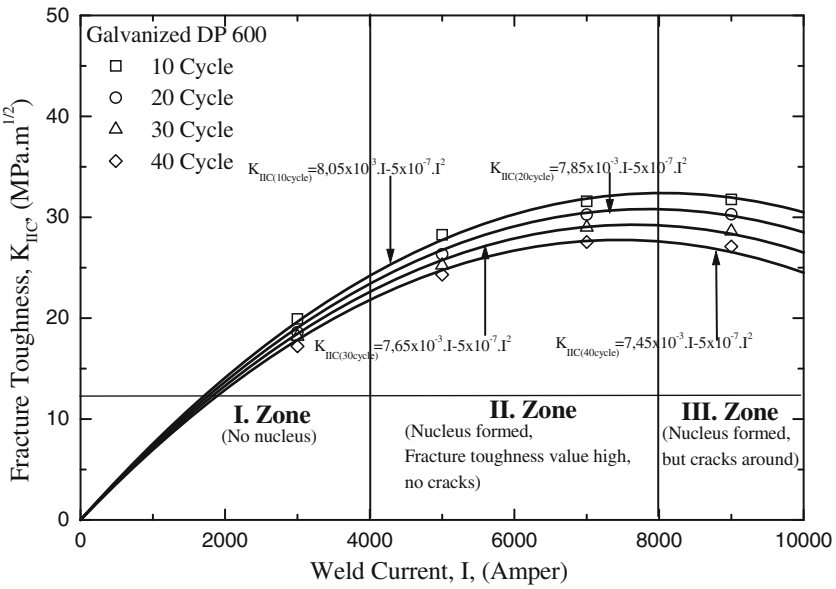

Fig. 7 Fracture toughness, K_{IIC}, versus weld current, I

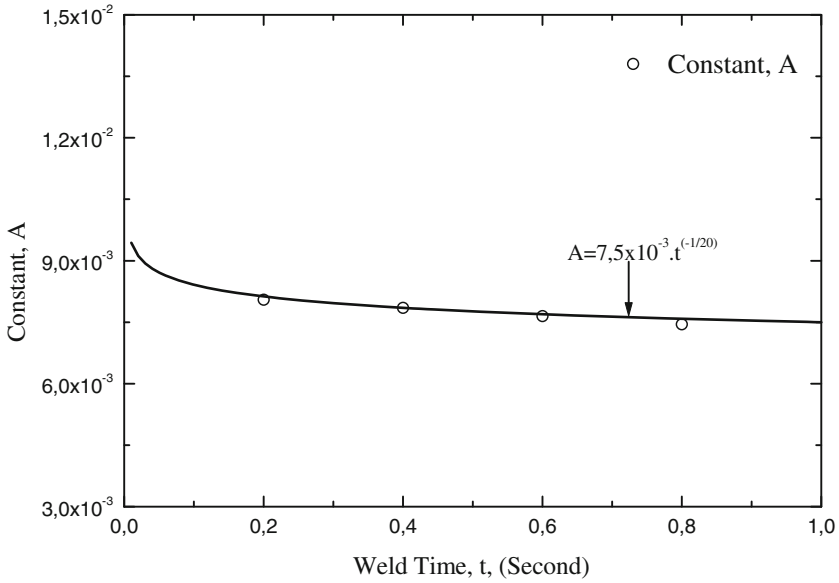

Fig. 8 Constant, A versus weld time, t

The criteria of identifying these three zones (Fig. 7):

1. Formation of weld nucleus
2. Fracture toughness value
3. Formation of micro crack around the weld nucleus

Based on these criteria:

Zone 1 is formed by the criteria of (1) and (2),
Zone 2 is formed by all the criteria
Zone 3 is formed by the criteria of (2) and (3).
The boundary of the zones are determined by using the obtained data

The fracture of spot weld occurs when the applied stress intensity factor at the crack tip is higher than the critical value. In this situation, the following relation can be used [18, 19]:

$$K_{\mathrm{II}} \geq K_{\mathrm{IIC}} \tag{2}$$

According to Fig. 7, the following second-degree relation can be used:

$$K_{\mathrm{IIC}} = I(A - BI) \tag{3}$$

where K_{IIC} is the fracture toughness of welding, A and B constants, I is the welding current.

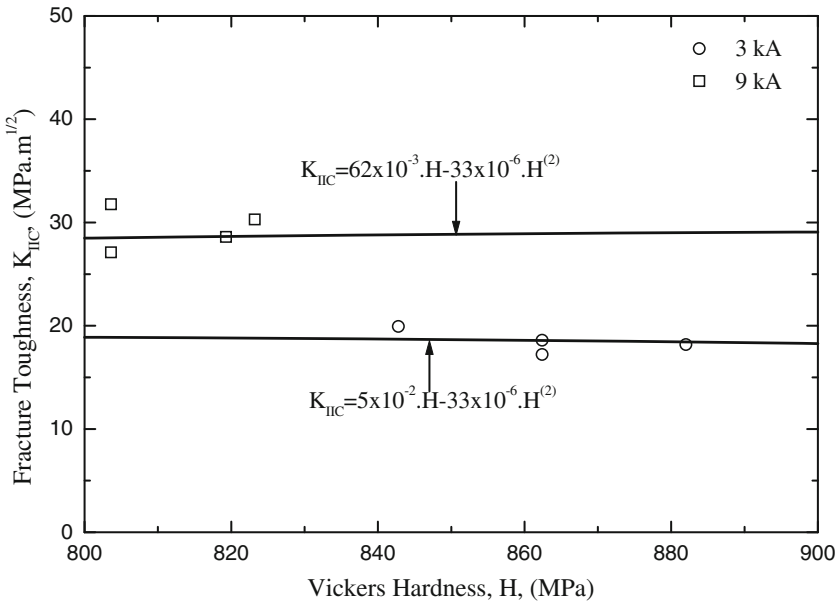

Fig. 9 Fracture toughness, K_{IIC}, versus Vickers hardness, H

Table 3 G and K constants in the variation of fracture toughness with hardness, H

Weld current I (kA)	The equations for K_{IIC}	Constant, G	Constant, K
3	$K_{IIC} = 62 \times 10^{-3}H - 33 \times 10^{-6}H^2$	62×10^{-3}	33×10^{-6}
9	$K_{IIC} = 5 \times 10^{-2}H - 33 \times 10^{-6}H^2$	5×10^{-2}	33×10^{-6}

The equations for different weld time values are given in Table 2. From Fig. 8, the A constants can be expressed in terms of welding time:

$$A = Et^{(-1/20)} \tag{4}$$

Where E=7.5×10^{-3} is a constant and t welding time in seconds.

Substituting (4) in (3), the following is obtained;

$$K_{IIC} = I\left[\left(Et^{(-1/20)}\right) - BI\right] \tag{5}$$

And substituting the values for constants, the following relation yields:

$$K_{IIC} = \frac{5I}{10^4}\cdot\left[\left(15t^{(-1/20)}\right) - \frac{I}{10^3}\right] \tag{6}$$

The variation of fracture toughness (K_{IIC}) with the Vickers hardness (H) is given in Fig. 9. The general fracture toughness equation can be written as follows:

$$K_{IIC} = H(G - KH) \tag{7}$$

where: K_{IIC} is the fracture toughness, G and K are constants, and H is the average hardness of weld nucleus.

The equations for different welding current values are given in Table 3. From Fig. 10, the G constants can be expressed in terms of welding current:

$$G = \frac{I^{(1/5)}}{10^2} \tag{8}$$

Where I is the welding current.

Substituting (8) for G and K from Table 3 in (7), the following equation can be written:

$$K_{IIC} = \frac{H}{10^2}\cdot\left[(I^{(1/5)}) - \frac{33.H}{10^4}\right] \tag{9}$$

It can easily be seen from (9) that the fracture toughness is dependent on welding current and the hardness of welded zone.

4 Discussion

The variables that affect the microstructure of the welding zone are welding current, the cycle of the current, holding time, the chemical composition of the steel sheets, and the cooling rate of the weld zone. Different microstructures arise depending on these parameters.

The heat required for these resistance welding processes is produced by the resistance of the work pieces to an electric current passing through the material. Because of the short electric current path in the work and limited weld time, relatively high welding currents are required to develop the necessary welding heat. The amount of heat generated depends upon three factors: (1) the amperage, (2) the resistance of the conductor, and (3) the duration of current. These three

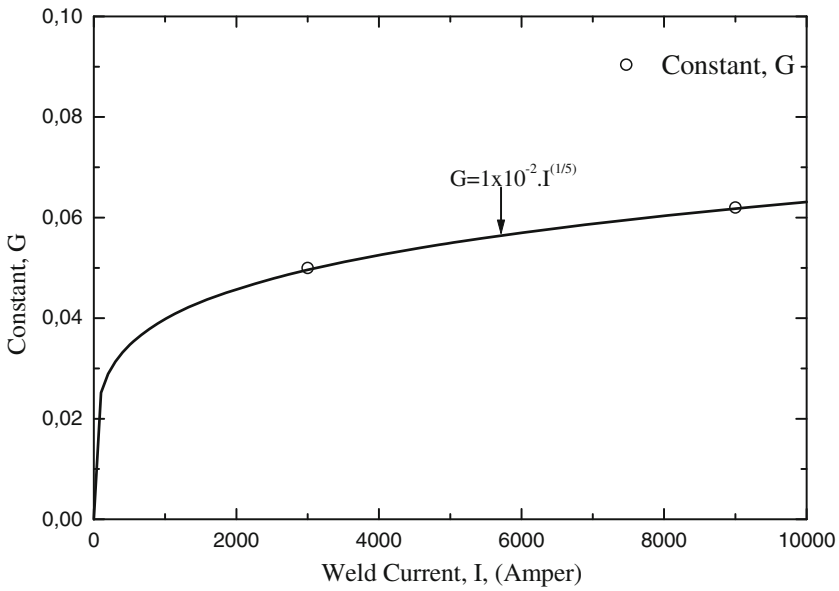

Fig. 10 Constant, G versus weld current, I

factors affect the heat generated as expressed in the formula [34, 35];

$$Q = I^2Rt \tag{10}$$

where Q is the heat generated (joule), I the current (ampere), R the resistance of the work (Ω), t is the duration of current (second).

The heat generated during the welding process is proportional to the square of current and welding time. The welding current and the welding time affect the amount of melting metal, microstructure, and diameter of weld nucleus. The welding current and time also affect the fracture toughness according to (6) and (9).

In this research, the obtained nugget diameter changes depending on weld time and weld current at the end of spot welding for examined specimen.

The fracture toughness is affected negatively if the welding current and the welding time are larger than critical values (Fig. 8) because the weld diameter decreases due to the excessive melting and splashing in the welding zone [12, 13, 36].

Nugget zone of the weld has similar properties to cast structure. Nugget zone has higher hardness than base material. The hardness of the martensitic structure in the welding zone can be given depending on the carbon rate in the alloy, as follows [37]:

$$H_M = 884.C\left(1 - C^2\right) + 294 \tag{11}$$

where H_M is the hardness of martensitic structure, and C is the carbon rate of the alloy.

The hardness can be estimated from (11) as H_M= 834 MPa. This value is in the measured hardness range of the welding zone. From this, it can be concluded that the welding nucleus changes completely into a martensitic structure.

The welding zone is hard and brittle due to the melt and cast-like structure. Depending on the cooling rate of the welded zone, shrinking and cold cracks form easily [2]. Due to this, coherent particles and grain boundaries are probable crack initiation sites. They could also aid crack propagation and eventually lead to failure in spot-welded joints [18, 19].

5 Conclusions

The following conclusions have been obtained for spot-weld joints made of sheet samples of galvanized DP600:

- The fracture toughness of the welded joint varies with the welding current and the welding time. This is a second-degree decreasing polynomial. In this variation, there are three zones:
  - I. Zone: The welding current and the welding time is insufficient to form the weld nucleus. The melting is less than the required value to form the nucleus.
  - II. Zone: The welding current and the welding time are sufficient for the nucleus formation. The fracture toughness is maximum in this zone. The weldability is maximum in this zone.
  - III. Zone: Extreme welding currents are present here. In this zone, the fracture toughness decreases despite the increase in welding current and welding time. The welded zone has the excessive melting and splashing.
- The fracture toughness decreases with welding current (Fig. 9).
- The fracture toughness of spot weld is not only dependent on the nugget diameter (D) but also depends on sheet thickness (S), tensile rupture force (F), welding time (t), and current (I).

Acknowledgments The authors would like to thank also Mr. Özcan on behalf of TOFAS AS in Turkey for their kindly materials supports.

References

1. Ozturk F, Toros S, Kilic S (2009) Tensile and spring-back behavior of DP600 advanced high strength steel at warm temperatures. J Iron Steel Res Int 16(6):41–46
2. Ma C, Chen DL, Bhole SD, Boudreau G, Lee A, Biro E (2008) Microstructure and fracture characteristics of spot-welded DP600 steel. Mater Sci Eng A 485:334–346
3. Xinsheng L, Xiaodong W, Zhenghongz G, Min W, Yixiong W, Younghua R (2010) Microstructures in a resistance spot welded high strength dual phase steel. Mater Char 61:341–346
4. Kleiner M, Chatti S, Klaus A (2006) Metal forming techniques for lightweight construction. J Mater Process Technol 177:2–7
5. Zhang XQ, Chen GL, Zhang YS (2008) Characteristics of electrode wear in resistance spot welding dual-phase steels. Mater Des 29:279–283
6. Hayat F, Demir B, Aslanlar S, Acarer M (2009) Effect of welding time and current on the mehanical properties of resistance spot welded IF (DIN EN 10130–11999) steel. Kov Mat 47:11–17
7. Hayat F, Demir B, Acarer M (2007) Tensile shear stress and microstructure of low-carbon dual phase Mn-Ni steels after spot resistance welding. M Sci Heat Treat 49:484–489
8. Bak A, Gunduz S (2009) Effect of strain ageing on the mechanical properties of ınterstitial free steels under as-received, heat treated and spot welded conditions for automotive applications. Proc Inst Mech Eng Part D-J Automob Eng 209:785–791
9. Erdogan M (2002) The effect of new ferit content on tensile fracture behaviour of dual-phase steels. J Mat Sci 37:3623–3630
10. Erdogan M (2003) The effect of austenite dispersion on phase transformation in dual phase steels. Scr Mater 48:501–508
11. I-CAR (2003) Porsche cayenne rocker panel sectioning change—A collision repair perspective. Technical information for the collision industry. (www.i-car.com)

12. AISI (2002) Steel technology roadmap automotive. AISI, Southfield, pp 1–95
13. Corus Research, Development & Technology (2008) Automotive Applications, Driving materials excellence: Material assessment for crash. Corus RD&T, IJmuiden
14. Hayat F (2011) The effects of the welding current on heat input, nugget geometry, and the mechanical and fractural properties of resistance spot welding on Mg/Al dissimilar materials. Mater Des 32:2476–2484
15. Kulekci MK, Mendi F, Sevim I, Basturk O (2005) Fracture toughness of friction stir welded joints of AlCu4SiMg aluminium alloy. Metalurgija 44:209–213
16. Shariati M, Maghrebi MJ (2009) Experimental study of crack growth behavior and fatigue life of spot weld tensile-shear specimens. J Appl Sci 9:438–448
17. Vural M, Akkus A (2004) On the resistance spot weldability of galvanized interstitial free steel sheets with austenitic stainless steel sheets. J Mater Process Technol 153–154:1–6
18. Sevim I (2005) Fracture toughness of spot-welded steel joints. Kov Mat 43:113–123
19. Sevim I (2006) Effect of hardness to fracture toughness for spot welded steel sheets. Mater Des 27:21–30
20. Pook LP (1975) Fracture mechanics analysis of the fatigue behavior of spot welds. Int J Fract 11:173–176
21. Paris PC, Sih GC (1965) On fracture toughness testing and its application, ASTM STP381. ASTM, Philadelpia, p30
22. Kassir MK, Sih GC (1968) Int J Fract Mech 41:347–353
23. Radaj D (1989) Strength assesment for spot-welded joints on the local stresses. Schweissen & Schneiden, Weld Cut 1:10–14
24. Zhang D (1997) Stress intensities at spot welds. Int J Fract 88:167–185
25. Zhang D (1999) Stress intensities derived from stresses around a spot weld. Int J Fract 99:239–257
26. Wilson B, Fine TE (1981) SAE technical paper series, paper no. 810354, p 1
27. Pan N, Sheppard SD (2003) Stress intensity factors in spot welds. Eng Fract Mech 70:671–684
28. Darwish SM, Soliman MS, Al-Fahead AM (1998) Manufacturing and characteristics of brass damping sheets. J Mater Process Technol 79:66–71
29. Chang B, Yaowu SY, Lu L (2001) Studies on the stress distribution and fatigue behavior of weld-bonded lap shear joints. J Mater Process Technol 108:307–313
30. Chandel RS, Garber S (1974) Mechanical and metallurgical aspects of spot-welded joints. Met Technol 1:418–424
31. Zuniga SM, Sheppard SD (1995) Determining the constitutive properties of the heat-affected zone in a resistance spot weld. Modeling Simul Mater Sci Eng A 3:391–416
32. Marya M, Gayden XQ (2005) Development of requirements for resistance spot welding dual-phase (DP600) steels part 1- the causes of interfacial fracture. Weld Res 11:172–182
33. Baltazar Hernandez VH, Kuntz ML, Khan MI, Zhou Y (2008) Influence of microstructure and weld size on the mechanical behaviour of dissimilar AHSS resistance spot welds. Sci Technol Weld Join 13:769–776
34. Aslanlar S (2006) The effect of nucleus size on mechanical properties in electrical resistance spot welding of sheets used in automotive industry. Mater Des 27:125–131
35. Kocabekir B, Kaçar R, Gündüz S, Hayat F (2008) An effect of heat input, weld atmosphere and weld cooling conditions on the resistance spot weldability of 316 L austenitic stainless steel. J Mater Process Technol 195:327–335
36. Vural M, Akkus A, Eryurek B (2006) Effect of welding nugget diameter on the fatigue strength of the resistance spot welded joints of different steel sheets. J Mater Process Technol 176:127–132
37. Khan MI, Kuntz ML, Biro E, Zhou Y (2008) microstructure and mechanical properties of resistance spot welded advanced high strength steels. Mater Tran 49:1629–1637